

# Structural and crystal-chemical characteristics of the apatite deposits from human aortic walls

SERGEI N. DANILCHENKO<sup>1</sup>, ALEKSEI N. KALINKEVICH<sup>1,\*</sup>, ROMAN A. MOSKALENKO<sup>2</sup>,  
VLADIMIR N. KUZNETSOV<sup>1</sup>, ALEKSANDR V. KOCHENKO<sup>1</sup>, EVGENIA V. HUSAK<sup>1,2</sup>,  
VADIM V. STARIKOV<sup>3</sup>, FUYAN LIU<sup>4</sup>, JUNHU MENG<sup>4</sup>, JINJUN LÜ<sup>5</sup>

<sup>1</sup>Institute for Applied Physics, NAS of Ukraine, Sumy, Ukraine

<sup>2</sup>Medical Institute of Sumy State University, Sumy, Ukraine

<sup>3</sup>Department of Metal Physics, National Technical University “Kharkov Polytechnic Institute”, Kharkov, Ukraine

<sup>4</sup>Lanzhou Institute of Chemical Physics, Chinese Academy of Sciences, Lanzhou, P. R. China

<sup>5</sup>Key Laboratory of Synthetic and Natural Functional Molecular Chemistry of the Ministry of Education, College of Chemistry and Materials Science, Northwest University, Xi’an, China

\*Corresponding author: Aleksei N. Kalinkevich; Institute for Applied Physics, NAS of Ukraine, 58 Petropavlovskaya St., Sumy 40000, Ukraine; Phone: +38 0542 333089; Fax: +38 0452 223760; E-mail: kalinkevich@gmail.com

(Received: June 6, 2017; Revised manuscript received: March 26, 2018; Accepted: April 23, 2018)

**Abstract:** Thermal behavior of biological apatite is the object of several studies. Crystal size, carbonate content, phase composition, and other parameters change during annealing up to 900 °C in biological minerals with apatite structure. The way these parameters change reflects the specific properties of the initial bioapatite. This work presents data on thermal transformations of pathological bioapatite from the human cardiovascular system, namely aortic wall deposits. Some minor elements, foreign to calcium hydroxyapatite (e.g., Na and Mg), can be both incorporated in the apatite structure and localized in the surface layers of crystals, modifying functions of the mineral. A new approach was proposed to determine the predominant location of minor elements, such as Mg, Na, and K, in the mineral of pathological deposits. Mg and Na in pathological apatite can be in both structurally bound (substituting calcium in lattice) and labile (localized on the crystal surface) states, while K is not able to join the apatite structure in significant amount or be chemically bound to it. This approach, based on atomic spectrometry, can be used effectively in combination with a set of traditional techniques, such as like EDS, IRS, and XRD.

**Keywords:** biomineralization, pathological mineralization, crystallization, electron microscopy, X-ray crystallography

## Introduction

Recent investigations [1, 2] and earlier works [3, 4] have shown that the mineral of cardiovascular pathological deposits consists of poorly crystalline carbonate-substituted apatite. However, the chemical diversity of biological apatites [5, 6] allows great variability in their reactivity and biological properties providing a unique adaptability to various biological roles. In this sense, “pathological” bioapatites, despite the established similarity with bone apatite [7–9], may have a number of specific features related to their mode of formation. In addition to chemical composition and structural characteristics, the morphological, microstructural, and ultrastructural features of the apatite in ectopic calcifications need further investigation, one of the important aims of which is the search for the systematic

correlations of these characteristics with the etiological aspects of the pathologies. Polymorphism [9–12] of crystal particles deposited in blood medium and on the surface of vessels and leaflets of heart valves attracts the great attention. Another specific characteristic of pathological bioapatites is the high value of Ca/P ratio, which, as reported in some papers [1, 9], significantly exceeds the ratio of the stoichiometric calcium apatite (1.67) and the typical ratios in bone and tooth materials (Table 3 in [13]). Currently, neither a functional role nor the sites of predominant location of excessive calcium in pathological mineral deposits with apatite-like structure are clear, and need further in-depth study.

In the studies of biological apatite of skeletal tissue, the procedure of sample annealing is often used in order to determine the temperature dependence of various

---

This is an open-access article distributed under the terms of the [Creative Commons Attribution-NonCommercial 4.0 International License](https://creativecommons.org/licenses/by-nc/4.0/), which permits unrestricted use, distribution, and reproduction in any medium for non-commercial purposes, provided the original author and source are credited, a link to the CC License is provided, and changes – if any – are indicated.

---

characteristics [14–18]. Usually, X-ray diffraction (XRD), infrared spectroscopy (IRS), and scanning electron microscopy (SEM) with X-ray microanalysis are applied for characterization of annealed material. Several sequential processes occurring during thermal treatment of biological apatite from mineralized tissues can be attributed to the following temperature ranges: (1) thermal decomposition and removal of the organic component and bound water in the temperature range of 400–600 °C; (2) recrystallization of bioapatite accompanied by the removal of  $\text{CO}_3^{2-}$  at the temperatures of 600–900 °C; and (3) bioapatite phase decomposition with the formation of other calcium phases [e.g., beta-tricalcium phosphate ( $\beta$ -TCP) and CaO] in the range from 900 to 1,200 °C, depending on the initial state of biominerals. The presence of Mg in the samples of synthetic and biogenic apatite leads during its thermal decomposition to the formation of the crystalline phase of  $\beta$ -tricalcium magnesium phosphate. Quantitative characteristics of this phase give information about the original content and localization of magnesium in biominerals [19].

From the results of several studies, it is known that the character of the temperature-dependent recrystallization of biological apatite clearly depends on the origin of a sample, i.e., its initial state, and reflects the specific chemistry of the bioapatite, especially the carbonate content [17, 18, 20]. It is reasonable to assume that this is caused by the energy state of crystal lattice, which depends on the level of imperfection and disorder in the structure of biominerals [21]. More ordered crystals (e.g., in mature bone) have much smaller lattice energy than low-mineralized apatites with numerous structural defects, substituted ions, and vacancies (immature or unhealthy bone). The increased initial energy level of lattice reduces the amount of energy required for recrystallization during annealing. Furthermore, due to their initially smaller size, the crystals of immature bone exhibit a greater surface-area-to-volume ratio and so a higher energy state. Thus, the recrystallization of less ordered and more defective crystals of bioapatite should start at lower temperatures compared to the crystals with more ordered and perfect structure. This is the motivation for the study of the temperature conversion of biological apatite in order to evaluate the level of its initial imperfection and substructural features. This study is complicated by the presence of organic components in mineralized tissues, serving as a template for the nucleation and crystal aging, and simultaneously spatially separating the individual crystals and their groups, limiting direct mechanical contacts. The lack of such contacts in low-mineralized tissues with high content of organic components prevents the rapid temperature-induced growth and agglomeration of crystals [14, 16–18]. Thus, during the annealing of biological mineralized tissues, one can specify two competing factors influencing the thermally activated processes: redundant structural

imperfections of the crystals, which accelerate the recrystallization, and the presence of organic matrix, which impairs the mass transport of mineral components, and finally agglomeration and fusion of the crystals.

An important feature of bioapatites is their high-temperature phase decomposition with the formation of two-phase and sometimes three-phase systems [16–18, 20, 22]. The analysis of the products of bioapatite's phase decomposition seems to be very informative in studying defects in the structure of natural samples, as confirmed by a number of relevant studies [19, 21, 23]. In fact, very small variations of the Ca/P ratio in the raw bioapatite lead to great changes in material composition and characteristics after thermal treatment.

Therefore, the study of the temperature behavior of biogenic apatites is of a considerable scientific interest and can significantly extend existing notions of structural and morphological features of pathological calcium phosphate deposits. The objective of this work was to study the structural, crystal-chemical, and morphological characteristics of the mineral of human cardiovascular system's pathological calcifications represented by aortic wall deposits. Special attention was paid to exploring the possibilities to obtain additional data by analyzing the effects of thermally activated reactions in biominerals. Furthermore, there are many fundamental publications devoted to the effects of heat treatment on bone apatite, whereas for "pathological" apatites, this approach was applied very limited so far.

## Materials and Methods

### *Sample preparation*

Samples were obtained from the Medical Institute of Sumy State University (Ukraine), where anatomical analysis, histomorphology, histochemistry, and medical morphometry of them have been performed.

### *Ethical approval*

The study was approved by the Medical Ethics Committee of the Regional Clinical Hospital of Sumy and Medical Institute of Sumy State University.

The investigated collection includes 21 specimens of calcified aortic walls (hereafter, the names of the samples are represented as AortaCalcIN, where *N* is the number of the specimen). After manual pretreatment (separation, cleaning, and drying), the samples were annealed in an electric furnace in air at a temperature of 200 °C for 1 h. This treatment guarantees the removal of free water and partial thermal decomposition of organic components [17]. On the other hand, the structure and ultrastructure of bioapatite remains unaffected after heating at 200 °C. Thus, such samples can be considered as original ones in terms of their

bioapatite state, but they are in much more suitable form for XRD and IRS examination than raw aorta tissues.

After first SEM and XRD observation, the material of the pathological deposits was subjected to annealing in the electric furnace at a temperature of 900 °C for 1 h in preparation for further examinations. For IRS, in addition, several specimens were annealed at an intermediate temperature (450 °C).

Atomic spectrometry (AS) was applied for the evaluation of the concentration of some elements in the “labile” (water soluble) state in contrast with the bulk content available from energy-dispersive spectroscopy (EDS). For AS analysis, the material of deposit was annealed at a temperature of 200 °C, homogenized by grinding in a mortar, and then divided into five roughly equal parts (~0.02/0.05 g). Each part was then annealed at one of the temperatures, 600, 640, 680, 720, and 760 °C, during 1 h. Here, the annealing temperatures were chosen, because in biogenic and synthetic apatite after 650–700 °C, the recrystallization with partial elimination of CO<sub>3</sub><sup>2-</sup> ions is observed [24]. In this temperature range, we revealed [25, 26] high mobility and migration activity of some ions.

After annealing, the powdered material was treated with ultrasonication (US; power density ≈ 15/20 W/cm<sup>2</sup>, peak output frequency ~22 kHz) for 10–15 min in distilled water in UZDN-A device (SELMI, Ukraine). The suspension obtained was filtered out. The elements concentration was measured in aqueous medium by the AS (“labile” fractions).

#### *Data acquisition and processing*

For our investigation, we selected those samples with adequate for analyzing a mineral fraction. The small amounts of the material did not always allow the application of all experimental techniques, which was a problem. That is why the extended study was applied to only a few samples, and only three samples were the objects of comprehensive analysis. XRD was the basic method of investigation, whereas AS examination after heating and subsequent ultrasonic treatment (US + AS) was tested as a new approach.

The inorganic material of aortic wall deposits in the initial state (after low temperature treatment at 200 °C) and after annealing at 900 °C was characterized by scanning electron microscopes JSM-5600LV and JSM-6701F (JEOL, Japan). The JSM-5600LV is coupled with an energy-dispersive X-ray spectrometer IE250 (Oxford Instrument, Lanzhou Institute of Chemical Physics, China) equipped with X-Max Silicon Drift Detector (SDD; the spectral resolution of 124 eV at Mn K $\alpha$ ) and an ultra-thin window; the active area of the SDD is 50 mm<sup>2</sup>. Each spectrum was acquired integrating the signals from a scanned area. The time of the spectrum acquisition was about 20 s. We do not apply conductive coatings for materials before EDS analysis. Altogether, this should provide reliable elemental identification and

acceptable semiquantitative evaluation of the materials' composition, including the light elements.

The procedure for evaluating the composition of the sample is based on the classical ZAF correction scheme for matrix effects by the external standard method (Z, A, F are the corrections for the atomic number effect, for absorption of the generated X-radiation, and for secondary X-ray fluorescence effect, respectively) [27]. We used stoichiometric hydroxyapatite as the reference sample. The homogeneity and morphology of the surface at the micrometer level and the electrical conducting properties satisfy the requirements for X-ray microanalysis reference samples.

Occasionally, SEM observation was performed using the apparatus REMMA102 (SELMI).

XRD investigations were performed using the diffractometer DRON4-07 (“Burevestnik,” Russia) connected to the computer-aided experiment control and data processing system. Ni-filtered CuK $\alpha$  radiation (wavelength: 0.154 nm) was used with a conventional Bragg–Brentano  $\theta$ – $2\theta$  geometry ( $2\theta$  is the Bragg's angle). The current and the voltage of the X-ray tube was 20 mA and 30 kV, respectively. Samples were measured in the continuous registration mode (at the speed of 1.0 °/min) within the  $2\theta$ -angle range from 10° to 60°. All data processing procedures were carried out using of the program package DIFWIN-1 (“Etalon PTC” Ltd., Russia). The separation of overlapping diffraction lines was done with the freeware program New\_Profile 3.4 (<http://remaxsoft.ru/>). Phase analysis was carried out by comparing the diffraction patterns from the investigated samples and the reference data JCPDS. From our previous experience, the sensitivity of the XRD analysis relating to phase identification (threshold of detectability) is about 3–4 wt. %. Semiquantitative evaluation of the crystallite size was derived from physical broadening of the line profiles using Scherrer's formula ignoring lattice microstrain, in the same way as in previous works (e.g., [9, 16]). Powdered polycrystalline NaCl was used as the reference material free of size and microstrain broadening.

IRS in the range of 4000–400 cm<sup>-1</sup> was recorded by a Spectrum-One FTIR spectrometer (Perkin Elmer, National Technical University “Kharkov Polytechnic Institute,” Kharkov, Ukraine). Before the measurements, the powdered samples were mixed with the KBr powder (2.5–3.0 mg of a sample per 300 mg of KBr) and pressed into tablets.

The concentration of mobile ionic species like Na, Mg, and K were measured in an aqueous medium after sonication by the atomic spectrometer KAS 120.1 (SELMI). The analytical system includes a double-beam spectrophotometer equipped with a deuterium device for background absorption correction. Mg was determined by flame atomic absorption spectroscopy, and Na and K by flame atomic emission spectroscopy using an air-acetylene flame in both the cases. The details of the apparatus and AS measurements are described in earlier publications [16, 26].

## Results and Discussion

### SEM-EDS

According to the results of SEM, pathological calcification samples annealed at 200 °C, in most cases, are agglomerates of mineral particles with a layered or lamellar morphology (Fig. 1a). In some cases, relatively large aggregates are found with evidence of oriented growth in their constituent plate-like particles (Fig. 1b). Some of such formations have a large size (up to several hundred micrometers) and are characterized by a smooth surface on one side and layered “fragile” transverse (relative to the smooth side) fractures (Fig. 1c). Often there are numerous small crystal particles adhering to these large plate-like crystals. However, this can be a consequence of preparative procedures when a fine-dispersed fraction is deposited on the surface of large crystals during the thermal and mechanical transformation of the starting material. Smooth surfaces of large crystalline particles (Fig. 1c) are probably formed by direct deposition on the organic component of the deposit or immediately onto the aorta wall. These results confirm the effectiveness of low-temperature combustion at 200 °C to obtain crystalline particles freed from residues of organic

component. The assumption of direct contact of the smooth surface of mineral deposits with the aortic wall requires further experimental studies, as does the question of preferential crystallographic orientation of the plate-like crystals.

Recrystallization changes in the morphology of the mineral are observed after annealing at 900 °C, when agglomerates of elongated crystals with random orientation are formed (Fig. 2a). It is quite obvious (considering the following X-ray data) that elongated crystals are hexagonal prisms of apatite with the crystallographic axis “c” directed along the longest dimension of the columnar crystals. This thermally activated transformation of morphology suggests that the original plate-like crystals, even if they are oriented and orderly aggregated into the dense blocks, are energetically unfavorable and have extremely high-specific surface area. It should be noted that alongside agglomerates of prismatic columnar crystals are groups of branched acicular crystals with a common center, observed in the deposit material annealed at 900 °C (Fig. 2b); the lamellar layered morphology of the crystals is partially preserved after annealing. At high magnification, the granular structure of large particles was clearly visible in some cases (Fig. 2c).

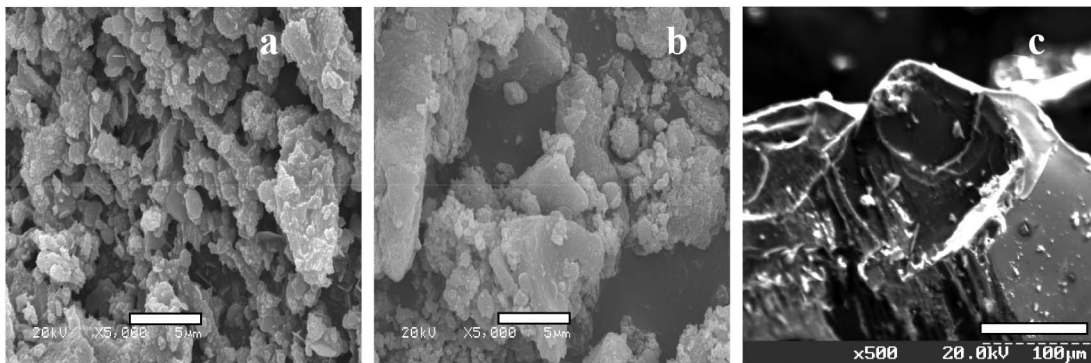


Fig. 1. SEM images of deposits particles from human aortic wall in initial state (annealed at 200 °C): (a) and (b) – (AortaCalc5), (c) – (AortaCalc9). Scale bars are 5 μm in the (a), 5 μm in the (b), and 100 μm in the (c)

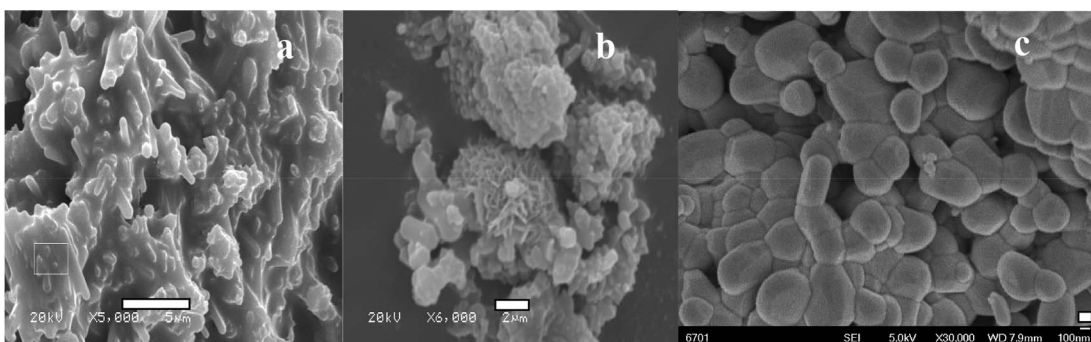


Fig. 2. SEM images of deposits crystal particles from human aortic wall after annealing at 900 °C: (a) and (b) – (AortaCalc3), (c) – (AortaCalc63). Scale bars are 5 μm in the (a), 2 μm in the (b), and 100 nm in the (c)



The study of the elemental composition of pathological calcifications of the aortic wall by EDS was carried out both by scanning of a representative portion of the surface of the material and by the local analysis of individual morphological details of special interest (e.g., the area marked with a white square in *Fig. 2a*).

In many cases, the EDS patterns show only intense Ca and P signals but with some trace additives (mostly Na and Mg); prominent C and O signals are also present in low-energy part of the spectra (*Fig. 3*). However, in a few cases, the signals from other elements (e.g., K, Cl, Fe, and S) are seen. Fe and S (as well as Mg, Zn, and some other elements) are usually found in the calcified and surrounding sites of aortas [28]. The dominant location of these elements is a debatable question; it is very probable that many of them can be both in the structurally bound state (substituting in apatite lattice) and in labile states (localizing on the crystal surfaces). Certainly, some of the listed elements could be residues from the low-volatilized organic compounds, e.g., Fe from the blood and S and Mg from organic tissue [29]. The estimation of Ca to P ratio shows that mainly it is higher than the standard value for stoichiometric calcium hydroxyapatite (1.67 at.). Generally, no specific distinctions have been discovered in the spectra of samples annealed at 900 °C comparing to the samples annealed at 200 °C.

Sample AortaCalc63, annealed at 900 °C, was subjected to more detailed examination. Observation of the low-energy part of the X-ray spectra (*Fig. 3*) shows that the C K $\alpha$  peak (0.277 KeV) cannot be substantially affected by neighboring Ca L $\alpha$  peak (0.341 KeV) due to sufficiently high-spectral resolution. Five EDS spectra from the same material were obtained (*Table I*). One aim of this study was to investigate the material's homogeneity. On the other hand, these results can serve as indices of the measurement reproducibility (on the assumption of chemical homogeneity of tested material). The data show that the element composition varies to a small extent between different parts of the mineral deposit. *Figure 4* represents the results of the EDS analysis: Na and Mg contents versus the variability of Ca/P ratio in the same mineral deposit. The apparent trend of decreasing Na concentrations with the increasing of Ca/P ratio should be mentioned. The highest Na content at the lowest Ca/P ratio may suggest that deficiency of calcium in apatite lattice can be partially compensated by Na [30, 31]. This correlation also indirectly confirms that some fraction of Na detected in materials belongs to apatite structure. Moreover, as it is proved by the simple calculation, the content of oxygen significantly exceeds the amount required for formation of apatite with the participation of available phosphorus. Even rough estimation shows that almost one quarter of the total oxygen may be present in other than apatite forms, probably in the crystal-bound water or be involved in other compounds with sodium, magnesium, calcium, and carbon. It is interesting to note

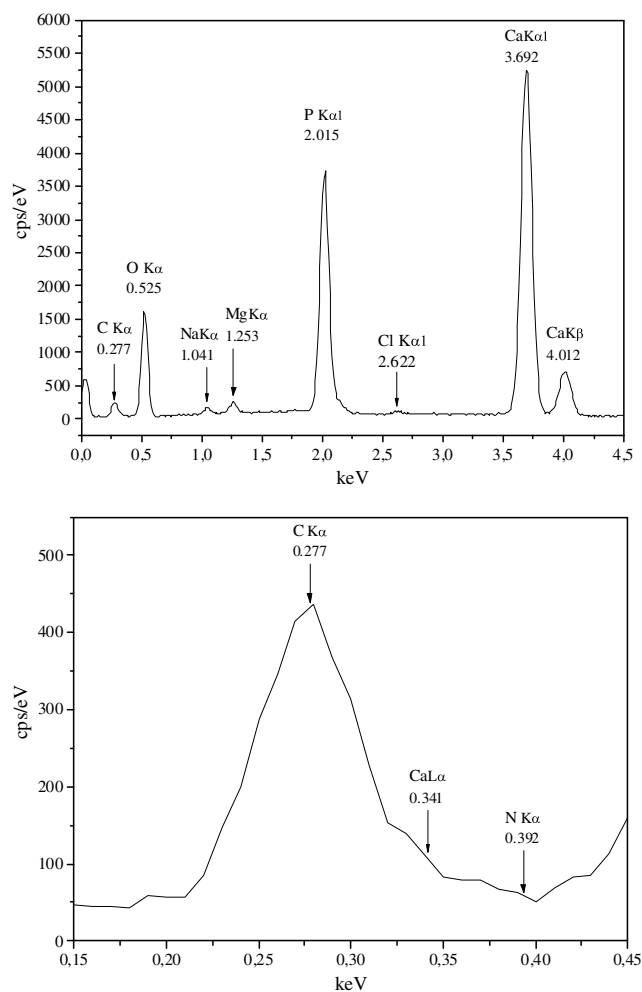


**Fig. 3.** Typical EDS spectrum of mineral deposit (AortaCalc63) annealed at 900 °C (above) and low-energy part of EDS spectrum for deposit (AortaCalc63) annealed at 900 °C (below)

that XRD pattern of this material annealed at 900 °C (sample AortaCalc63) has shown only the peaks of ordinary calcium hydroxyapatite,  $\text{Ca}_{10}(\text{PO}_4)_6(\text{OH})_2$  (JCPDS 9-432), also indicating very low degree of Na and Mg substitution for Ca. Therefore, the elements not belonging to conventional apatite structure (foreign to stoichiometric calcium hydroxyapatite) do not form detectable crystal phases and most likely exist in the chemical compounds (oxides, carbonates, and carbide) dispersed in the material or localized on the surface of apatite crystals.

In general, the EDS data have shown significant chemical inhomogeneity of the deposit material, while their averaged Ca/P ratio is very close to stoichiometric value (*Fig. 4*).

#### XRD

The XRD patterns of the initial samples (the samples after low temperature ashing at 200 °C) show the presence of

**Table I** The data of EDS analysis of material from same sample (AortaCalc63) subjected to the annealing under the temperature of 900 °C (results of five measurements with the averaging)

	C		O		Na		Mg		P		Cl		Ca	
	wt. %	at. %	wt. %	at. %	wt. %	at. %	wt. %	at. %	wt. %	at. %	wt. %	at. %	wt. %	at. %
1	4.02	7.31	43.64	59.56	3.93	3.74	1.17	1.05	16.28	11.47	-	-	30.97	16.87
2	4.40	8.10	43.66	60.29	0.70	0.68	0.73	0.67	14.99	10.69	0.21	0.13	35.30	19.45
3	5.29	9.53	44.96	60.78	0.39	0.36	0.63	0.56	15.42	10.77	0.27	0.16	33.05	17.84
4	4.17	8.21	43.27	63.45	0.65	0.66	0.72	0.69	16.08	12.18	0.21	0.14	36.07	20.87
5	3.53	6.22	44.05	63.53	2.71	2.72	1.07	1.01	16.37	12.19	0.33	0.21	34.64	20.03
av.	4.28	7.87	43.92	61.52	1.68	1.63	0.86	0.80	15.83	11.46	0.20	0.13	34.0	19.0
$\sigma_{n-1}$	0.647	1.220	0.645	1.848	1.566	1.508	0.240	0.220	0.598	0.728	0.124	0.078	2.029	1.631

$\sigma_{n-1}$ : variance about mean (average squared error). The values represented in this table are only qualitative, i.e., to be viewed as relative, not absolute values; for example, to estimate the Ca/P ratio or proportion of some elements

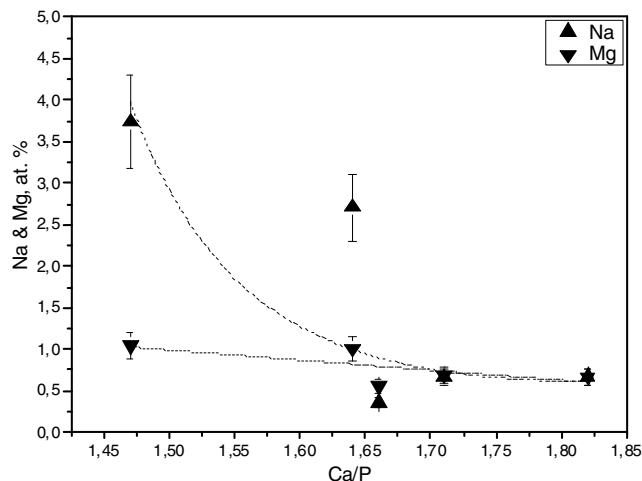


**Fig. 4.** Na and Mg contents versus the variability of Ca/P ratio in the same sample, AortaCalc63 (for stoichiometric calcium hydroxyapatite Ca/P=1.67 at. %). The dashed lines are drawn only to indicate general tendency

poorly crystalline apatite with some variation in crystallinity degree, as indicated by peak width (Fig. 5). The diffraction pattern of hydroxyapatite from a database (JCPDS 9-432) is marked by vertical lines along the  $x$  axis. Rough estimation of main diffraction lines' profile width shows that the crystallite (crystal domain) size of apatite in aortic wall deposits is comparable to the size of bone tissue bioapatite crystallites (~20 nm) [15, 16]. It should be noted that XRD data of the initial samples are not of sufficient resolution to allow quantitative characterization of the mineral, e.g., it is impossible to determine the cell parameters with sufficient accuracy or to detect the traces of other phases.

After the annealing of calcified deposits at a temperature of 900 °C for 1 h, recrystallization of apatite crystals was observed. In some cases,  $\beta$ -TCP (mainly JCPDS 9-169) or CaO (JCPDS 37-1497) phases were revealed in addition to apatite (Fig. 5). The admixture of CaO was found in four samples; whereas  $\beta$ -TCP was only found in 3 of 21 samples; in a single case, the presence of  $\text{NaCaPO}_4$  was clearly recognized. Formation of two-phase system "apatite +  $\beta$ -TCP" indicates Ca deficiency in the initial nanocrystalline apatite compared to stoichiometric hydroxyapatite, whereas "apatite + CaO" (or "apatite +  $\text{NaCaPO}_4$ ") biphasic mixture denotes calcium excess in pathological mineral deposits with apatite structure. For illustration, according to the reference [32], if molar Ca/P ratio in a synthesized apatite is 1.71, the heated material contains 1.5 wt. % of CaO in addition to apatite phase. On the other hand, even little Ca deficiency in initial apatite (Ca/P = 1.66) leads to the formation of a few wt. % of  $\beta$ -TCP at a temperature of 1,000 °C. Therefore, it seems that the XRD phase analysis of annealed samples is a fine stoichiometric-sensitive approach for calcium hydroxyapatite. According to the XRD analysis, we can conclude that

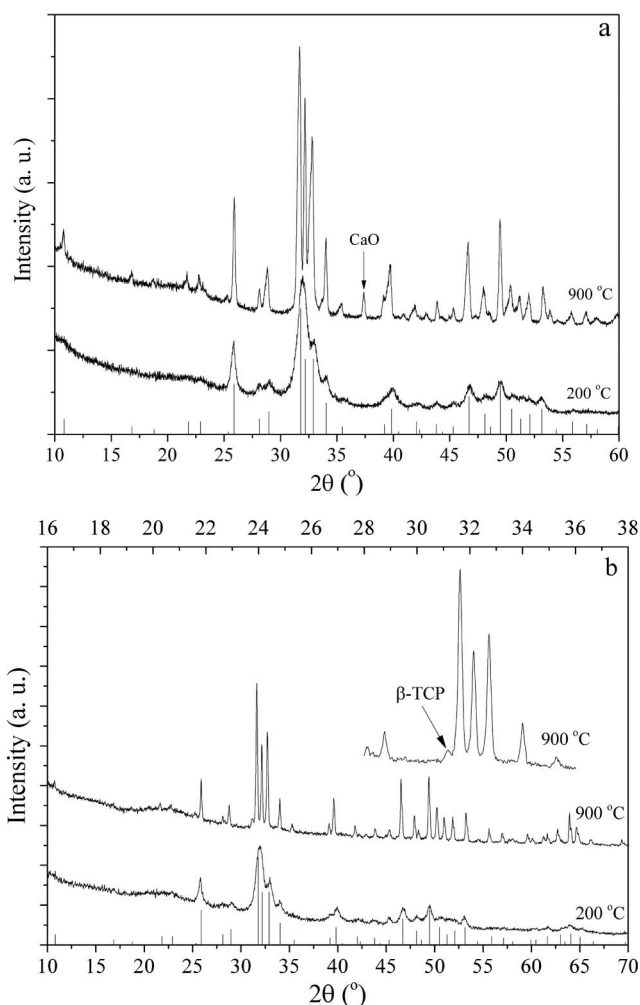


**Fig. 5.** X-ray diffraction patterns of human aorta deposits annealed at 200 °C and at 900 °C with the evidence of the CaO (a: sample AortaCalc5) or  $\beta$ -TCP (b: sample AortaCalc17) formation. The asterisks mark the major peak of  $\beta$ -TCP or CaO; the upper scale of diffraction angle (b) corresponds to the inserted fragment of diffraction pattern. At the bottom, there is the theoretical pattern of hydroxyapatite according to JCPDS 9-432

the aortic wall apatite deposits both can be deficient in Ca and enriched with Ca compared to apatite, or have “normal” apatite stoichiometric Ca/P ratio. This assumption could be true in case of the absence of Ca-containing component on the surface of apatite crystals (e.g.,  $\text{CaCO}_3$  in non-apatitic environments or hydrated surface layer [33, 34]). With the sufficient amount of  $\text{CaCO}_3$  on crystal surface, the thermal destruction may lead to  $\text{CO}_2$  elimination and subsequent penetration of the released Ca into lattice vacancies. Moreover, the formation of CaO as a trace phase can occur under the favorable conditions for mass transfer. We suppose that formation of CaO or  $\beta$ -TCP under annealing not depend only on Ca excess or Ca deficiency in original apatite crystals, but also is determined by peculiarities in chemical composition of surface layer and specific surface of crystals or surface-area-to-volume ratio.

It was established by careful XRD phase analysis of the annealed samples with the selection of the most suitable phases of apatite family from a database, that, in several cases, the formed apatite phases were not the ordinary calcium hydroxyapatite,  $\text{Ca}_{10}(\text{PO}_4)_6(\text{OH})_2$  (JCPDS 9-432), but more complex phases of the apatite family with various isovalent and heterovalent substitutions in the anionic and cationic sublattice, e.g., calcium sodium magnesium phosphate apatite (JCPDS 89-6449). This indicates that the total mineral component of calcified deposits contained some elements foreign to stoichiometric hydroxyapatite. The presence of these elements in the apatite lattice of initial pathological calcifications was also possible, but to validate this, we should exclude the interphase migration of the elements during high-temperature treatment.

However, it can be concluded that the XRD analysis of annealed samples of bioapatite can provide valuable information about initial crystal-chemical characteristics of pathological apatite. For this, the XRD data should be combined with the information about the dominant location of some minor elements like Mg, Na, and K; in addition, the location of carbonates should be used.

The serious limitation of XRD is the averaged readings. Even with the smallest possible (in wide-angle XRD) cross section of the probing X-ray beam, the probed area of a sample contains many diverse elements in a complicated system. Moreover, XRD is not sensitive enough to detect ion substitutions in the lattice, if the ionic radii of the substitutes are close to the radii of the host ions. That is why, for the annealed AortaCalc63 sample, we have seen only the phase of hydroxyapatite, while EDS data revealed a rather wide spread in Ca/P ratio around the stoichiometric value.

### IRS

Typical examples of IR absorption spectra of calcified deposit on aortic walls annealed at 450 and 900 °C are shown in Fig. 6. In general, the spectra display the patterns associated with carbonate-substituted apatite [30, 35]. The bands at 1,000–1,100 and 500–600  $\text{cm}^{-1}$  correspond to different modes of  $\text{PO}_4$  group in apatite (the phosphate-stretching vibrations and phosphate-bending vibrations, correspondingly), whereas the bands at 2,840–2,960  $\text{cm}^{-1}$  can originate from  $\text{HPO}_4$  group [7, 30]. The narrow band at 3,570  $\text{cm}^{-1}$  can be assigned to hydroxyl groups present in the structure of apatite. The bands at 1,420–1,550 and 870–880  $\text{cm}^{-1}$  are derived from carbonate ions in the apatite structure [35].

The heating of the material to 450 °C is aimed to eliminate the contribution of main organic components and surface water. Comparison of the spectra at 450 and 900 °C should provide information about structural alteration of bioapatite in the process of recrystallization,

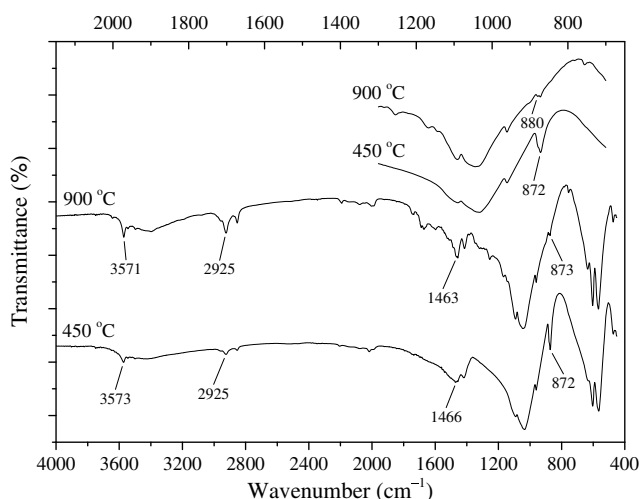


**Fig. 6.** Typical FTIR spectra of the aorta deposits annealed at 450 °C and 900 °C showing of carbonated components. The upper scale corresponds to the inserted fragments of the spectra

particularly about carbonate transformation and release. The first spectrum is typical for apatite containing B-type carbonate ( $\text{CO}_3\text{-for-PO}_4$ ) [30] with prominent  $\text{CO}_3^{2-}$ -bending vibration observed at  $872\text{ cm}^{-1}$ . After annealing at 900 °C, the intensity of this peak decreases appreciably, whereas the intensity of  $\text{CO}_3^{2-}$ -stretching vibrations at  $1,473\text{ cm}^{-1}$  and around  $1,418\text{ cm}^{-1}$  significantly increases. The IRS data obtained reveal that even after annealing at 900 °C, the apatite of deposits on aortic wall contains substantial amounts of  $\text{CO}_3^{2-}$  ions in both OH and  $\text{PO}_4$  positions. However, the mineral in the deposit at its initial state is more close to B-type carbonate apatite. Furthermore, the narrowing of the IR absorption bands in the temperature interval from 450 to 900 °C indicates improvement of apatite crystallinity during recrystallization and wholly conforms to the XRD data. The signal from  $\text{HPO}_4$  around  $2,920\text{ cm}^{-1}$  can be associated with Na for Ca substitution and/or Ca vacancy in the apatite lattice, since the presence of hydrogen phosphate substituting for  $\text{PO}_4$  is necessary for maintaining electrical charge balance.

## AS

It should be emphasized again that the data of EDS analysis (Table I) reveal the total concentrations of elements, not differentiated into fractions corresponding to apatite or to other chemical compounds. These chemical compounds could be free ions of metals or oxides, salts, carbonates, and carbides or belong to minor crystal phases if they are found. Because apatite solubility is negligibly small at normal conditions, non-lattice elements (ions and compounds) can be removed to aqueous solution, keeping the apatite structure unaffected, and

then their concentration can be determined by atomic spectroscopy. For this, we used annealing and subsequent US as described in “Methods” section. We believe that the values determined this way correspond to the “labile” fraction, although we suppose that not all labile ions can be transferred to aqueous medium after sonication, and so real concentrations of them may be higher. Therefore, the represented values have only indicative meaning. Nevertheless, comparing the data of EDS (Table I) and AS (Fig. 7) for the same sample AortaCalc63, we can deduce that the main part of Na (almost 3/4) and dominant fraction of Mg (up to 9/10) could not be removed to aqueous medium and therefore are in bound state. The concentration of potassium determined by AS (about 0.05 wt. %) is near the detection limit of EDS analysis, and so it was discovered by EDS only in few cases as a trace element. Probably, the amount of K determined by AS represents almost total content of K in the material. This observation supports the idea that K is mainly present in biological mineral in labile state (being localized on the crystal surface).

Small variability of Mg and K in examined temperature range (Fig. 7) suggests low migration activity of these ions. On the contrary, Na shows the tendency to the mass transfer. Particularly, at 720 °C, Na leaves the crystals, while when the annealing temperature is increased to 760 °C, the amount of Na in crystals grows. It could be connected with the reversible exchange of  $\text{CO}_3^{2-}$  ions [30] and rather well conforms to the IR spectra of annealed aorta wall deposit.

Some limitations of the tested approach need to be mentioned. We were unable to evaluate the contributions to the “labile” fraction from different sources and separate portions corresponding to surface-localized

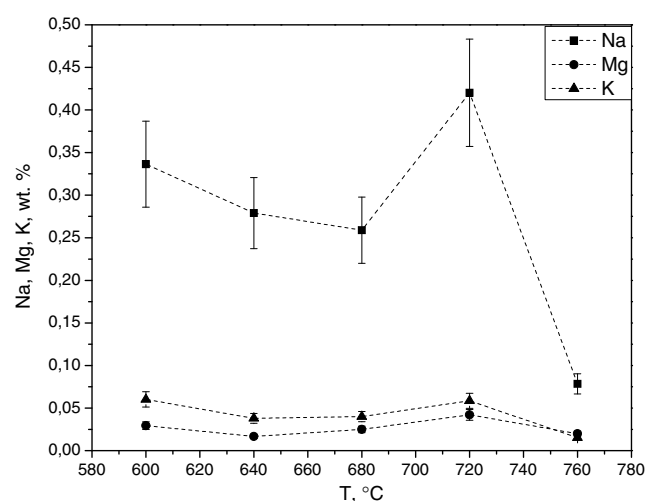


**Fig. 7.** Concentrations of Na, Mg, and K in water medium after ultrasonication of annealed and powdered sample AortaCalc63 (“labile” fraction of minor elements). The lines are drawn only to guide the eye



water-soluble compounds and associated with the remains of organic matrix. Further studies are needed to establish the predominant location of Na, K, and Mg (as well as some other elements), which can be both in structurally bound state and in labile states (localized on the crystal surface), or can belong to organic component of pathological deposit.

## Conclusions

A set of instrumental techniques (SEM-EDS, IRS, and XRD) was applied to characterize human aortic wall deposits in their initial state (after low-temperature combustion at 200 °C) and annealed at high temperature. Moreover, the new approach was tested to determine the “labile” fraction of such minor elements as Mg, Na, and K: AS analysis of aqueous medium after US of annealed mineral. In fact, the simple mechanical separation was used to compare the element concentrations in the whole material (EDS data) and in its “labile” component (AS data).

As the data have shown, the mineral of aortic wall deposits is apatitic but with a wide variety of defects and ionic substitutions. In addition to foreign ions located in lattice, there are some ions and compounds with surface localization. The EDS and AS combined results suggest that Mg and Na in pathological apatite can be both in structurally bound (substituting calcium in lattice) and in labile (localized on the crystal surface) states, whereas K is not able to join the apatite structure in significant amount or be chemically bound to it. The results of the work infer that EDS data [e.g., elements ratio Ca/P, (Ca + Mg + Na)/P] coupled with XRD phase analysis may provide valuable information on phase purity of pathological bioapatite and probable presence of the chemical components (oxides and carbonates) not forming separate crystal phases. However, here, the estimation of contribution from labile fraction of elements (including Ca) in total content is very important.

The thermal migration of carbonates in apatite can be identified by several instrumental techniques (first of all, IRS), while the delocalization of minor elements cannot be recognized easily. In particular, XRD pattern of initial bioapatite does not provide the information about lattice substitutions because of peak broadening and overlapping. Structural data on annealed apatite can give this information, but original localization of these elements is debatable due to the possibility of migration. Here, we propose a rather simple and effective approach to evaluate predominant location and migration ability of some “labile” ions in biological apatites. Our results show that there is a potential for the development of new methods to analyze thermal transformation of bioapatite and migration of the ions and groups including partial elimination of carbonate species. Further investigation is

required in order to fully understand the biological effects of structural imperfections and surface-localized mobile ionic species in pathological bioapatite. The systematic correlations of these features with the etiological aspects of pathologies are yet to be studied.

\* \* \*

**Funding sources:** This research was partially supported by the Ukrainian State Agency for science, innovation and informatization (grant no. 0113U005095) and by Chinese Academy of Sciences (program CU01-04) within the bilateral project “Ultrastructural organization, crystal-chemical characteristics and morphological transformation of nanostructured calcium phosphate in pathological deposits from human cardiovascular system”.

**Authors’ contribution:** SND: idea, manuscript design, article writing, and revising. ANK: manuscript design and SEM data analysis. RAM: idea and sample preparation. VNK: XRD data analysis. AVK: XRD measurements. EVH: AS measurements. VVS: IRS measurements. FL and JM: SEM measurements. JL: manuscript design, article writing, and revising.

**Conflict of interest:** The authors declare no conflict of interest.

**Acknowledgements:** The authors are grateful to Mr. Zhao Jiazheng from Lanzhou Institute of Chemical Physics for assistance with SEM-EDS techniques.

## References

- Cottignoli V, Cavarretta E, Salvador L, Valfré C, Maras A: Morphological and chemical study of pathological deposits in human aortic and mitral valve stenosis: A biominerological contribution. *Pathol Res Int* 2015, 342984 (2015)
- Cottignoli V, Relucanti M, Agrosi G, Cavarretta E, Familiari G, Salvado L, Maras A: Biological niches within human calcified aortic valves: Towards understanding of the pathological biomineralization process. *BioMed Res Int* 2015, 542687 (2015)
- Tomazic BB: Physiochemical principles of cardiovascular calcification. *Zeitschrift für Kardiologie* 90, 68–80 (2001)
- Stork L, Müller P, Dronskowski R, Ortlepp JR: Chemical analyses and X-ray diffraction investigations of human hydroxyapatite minerals from aortic valve stenosis. *Zeitschrift für Kristallographie* 220, 201–205 (2005)
- Rey C, Combes C, Drouet C, Sfihi H: Chemical diversity of apatites. *Adv Sci Technol* 49, 27–36 (2006)
- Rey C, Combes C, Drouet C, Lebugle A, Sfihi H, Barroug A: Nanocrystalline apatites in biological systems: Characterisation, structure and properties. *Materialwissenschaft und Werkstofftechnik* 38, 996–1002 (2007)
- Mangialardo S, Cottignoli V, Cavarretta E, Salvador L, Postorino P, Maras A: Pathological biominerals: Raman and infrared studies of bioapatite deposits in human heart valves. *Appl Spectrosc* 66, 1121–1127 (2012)
- Zeman A, Šmid M, Havelcova M, Coufalova L, Kučková Š, Velčovska M, Hynek R: The structure and material composition of ossified aortic valves identified using a set of scientific methods. *J Asian Earth Sci* 77, 311–317 (2013)
- Danilchenko SN, Kuznetsov VN, Stanislavov AS, Kalinkevich AN, Starikov VV, Moskalenko RA, Kalinichenko TG, Shang J, Lu JJ, Yang S: The mineral component of human cardiovascular deposits: Morphological, structural and crystal-chemical characterization. *Cryst Res Technol* 48, 153–162 (2013)

10. Wu CY, Martel J, Young D, Young JD: Fetuin-A/albumin-mineral complexes resembling serum calcium granules and putative nanobacteria: Demonstration of a dual inhibition-seeding concept. *PLoS One* 4, 1–32 (2009)
11. Prieto RM, Gomila I, Söhnel O, Costa-Bauza A, Bonnin O, Grases F: Study on the structure and composition of aortic valve calcific deposits. Etiological aspects. *J Biophys Chem* 2, 19–25 (2011)
12. Marra SP, Daghlian C.P, Fillingier MF, Kennedy FE: Elemental composition, morphology and mechanical properties of calcified deposits obtained from abdominal aortic aneurysms. *Acta Biomater* 2, 515–520 (2006)
13. Elliott JC (2002): Calcium phosphate biominerals. In: *Phosphates: Geochemical, geobiological, and materials importance*, Reviews in Mineralogy and Geochemistry, eds Kohn MJ, Rakovan J, Hughes JM, Mineralogical Society of America, Chantilly, pp. 427–453
14. Etok SE, Valsami-Jones E, Wess TJ, Hiller JC, Maxwell CA, Rogers KD, Manning DAC, White ML, Lopez-Capel E, Collins MJ, Buckley M, Penkman KEH, Woodgate SL: Structural and chemical changes of thermally treated bone apatite. *J Mater Sci* 42, 9807–9816 (2007)
15. Rogers KD, Daniels P: An X-ray diffraction study of the effects of heat treatment on bone mineral microstructure. *Biomaterials* 23, 2431–2622 (2002)
16. Danilchenko SN, Koropov AV, Protsenko IY, Sulkio-Cleff B, Sukhodub LF: Thermal behavior of biogenic apatite crystals in bone: An X-ray diffraction study. *Cryst Res Technol* 41, 268–275 (2006)
17. Mkukuma LD, Skakle JMS, Gibson IR: Effect of the proportion of organic material in bone on thermal decomposition of bone mineral: An investigation of a variety of bones from different species using thermogravimetric analysis coupled to mass spectrometry, high-temperature X-ray diffraction, and Fourier transform infrared spectroscopy. *Calcif Tissue Int* 75, 321–328 (2004)
18. Greenwood C, Rogers K, Beckett S, Clement J: Initial observations of dynamically heated bone. *Cryst Res Technol* 48, 1073–1082 (2013)
19. Danilchenko SN, Protsenko IY, Sukhodub LF: Some features of thermo-activated structural transformation of biogenic and synthetic Mg-containing apatite with  $\beta$ -tricalcium-magnesium phosphate formation. *Cryst Res Technol* 44, 553–560 (2009)
20. Becker A, Epple M, Müller KM, Schmitz I: A comparative study of clinically well-characterized human atherosclerotic plaques with histological, chemical, and ultrastructural methods. *J Inorg Biochem* 98, 2032–2038 (2004)
21. Greenwood C, Rogers K, Beckett S, Clement J: Bone mineral crystallisation kinetics. *J Mater Sci Mater Med* 23, 2055–2060 (2012)
22. Tomoaia Gh, Mocanu A, Vida-Simiti I, Jumate N, Bobos L-D, Soritau O, Tomoaia-Cotisel M: Silicon effect on the composition and structure of nanocalcium phosphates. In vitro biocompatibility to human osteoblasts. *Mater Sci Eng C* 37, 37–47 (2014)
23. Kato Y, Ogura H: Mineral phase in experimental ectopic calcification induced by lead acetate in the rat. *Calcif Tissue Res* 25, 69–74 (1978)
24. Danilchenko SN, Pokrovskiy VA, Bogatyr'ov VM, Sukhodub LF, Sulkio-Cleff B: Carbonate location in bone tissue mineral by X-ray diffraction and temperature-programmed desorption mass spectrometry. *Cryst Res Technol* 40, 692–697 (2005)
25. Danilchenko SN, Kulik AN, Pavlenko PA, Kalinichenko TG, Buhay OM, Chemeris II, Sukhodub LF: Thermally activated diffusion of magnesium from bioapatite crystals. *J Appl Spectrosc* 73, 437–443 (2006)
26. Danilchenko SN: The approach for determination of concentration and location of major impurities (Mg, Na, K) in biological apatite of mineralized tissues. *J Nano Electron Phys* 5, 03043 (2013)
27. Goldstein JI, Yakowitz H (1975): *Practical scanning electron microscopy. Electron and ion microprobe analysis*. Plenum Press, New York/London
28. Tohno S, Tohno Y, Minami T, Moriwake Y, Azuma C, Ohnishi Y: Elements of calcified sites in human thoracic aorta. *Biol Trace Elem Res* 86, 23–30 (2002)
29. Li Z, Pasteris JD: Chemistry of bone mineral, based on the hypermineralized rostrum of the beaked whale *Mesoplodon densirostris*. *Am Mineral* 4, 645–653 (2014)
30. Elliott JC (1994): *Structure and chemistry of the apatites and other calcium orthophosphates*. Elsevier, Amsterdam.
31. LeGeros RZ: Apatites in biological-systems. *Prog Crystal Growth Characterization Mater* 4, 1–45 (1981)
32. Raynaud S, Champion E, Bernache-Assollant D, Thomas P: Calcium phosphate apatites with variable Ca/P atomic ratio I. Synthesis, characterisation and thermal stability of powders. *Biomaterials* 23, 1065–1072 (2002)
33. Cazalbou S, Combes C, Eichert D, Rey C: Adaptive physico-chemistry of bio-related calcium phosphates. *J Mater Chem* 14, 2148–2153 (2004)
34. Rey C, Combes C, Drouet C, Cazalbou S, Grosse D, Brouillet F, Sarda S: Surface properties of biomimetic nanocrystalline apatites; applications in biomaterials. *Prog Crystal Growth Characterization Mater* 60, 63–73 (2014)
35. Markovic M, Fowler BO, Tung MS: Preparation and comprehensive characterization of a calcium hydroxyapatite reference material. *J Res Natl Inst Stand Technol* 109, 553–568 (2004)